Available online at www.sciencedirect.com
SCIENCE DIRECT®
Journal of Power Sources 148 (2005) 1–8
JOURNAL OF POWER SOURCES
www.elsevier.com/locate/jpowsour

Enhancement effect of an adsorbed organic acid on oxygen reduction at various types of activated carbon loaded with platinum

Jun Maruyama *, Ikuo Abe

Environmental Technology Department, Osaka Municipal Technical Research Institute, 1-6-50 Morinomiya, Joto-ku, Osaka 536-8553, Japan

Received 25 October 2004; received in revised form 20 December 2004; accepted 25 January 2005
Available online 18 March 2005

Abstract

We have found that application of activated carbon as a support of platinum in electrocatalysts for polymer electrolyte fuel cells improves the activity for oxygen reduction, especially by using activated carbon with trifluoromethanesulfonic acid adsorbed in the pores. In the present study, we investigated this enhancement effect of the acid for oxygen reduction at activated carbon of various specific surface areas and mean pore diameters. After adsorption of potassium trifluoromethanesulfonate onto the activated carbon loaded with platinum, a catalyst layer was formed from the activated carbon and a polymer electrolyte, followed by replacing the potassium ions with protons. We measured the adsorption isotherms of trifluoromethanesulfonate onto the activated carbons and found that adsorption behavior was dependent on the kind of activated carbon. Electrochemical properties of the layer was evaluated by cyclic voltammetry and by the relationship between electrode potential and oxygen reduction current in perchloric acid solution, supporting the layer on a rotating glassy carbon disk electrode. The properties, and consequently the enhancement effect of the organic acid for oxygen reduction, were clearly dependent on the kind of activated carbon and were explicable based on the pore structure and the adsorption behavior.

Keywords: Polymer electrolyte fuel cell; Oxygen reduction; Activated carbon; Pore structure; Organic acid; Adsorption

1. Introduction

Voltage loss in the polymer electrolyte fuel cell (PEFC) is mainly caused by the large overpotential for cathodic oxygen reduction [1] and has to be remedied by development of active electrocatalysts. Currently, an electrocatalyst consisting of highly dispersed platinum particles supported on carbon black (Pt/C) is used [2–7], mixed with perfluorosulfonate ion-exchange resin to form a catalyst layer in the electrode. The diameter of the dispersed Pt particles is 1–5 nm, giving them a large specific surface area (50–200 $m^2\ g^{-1}$) greater than that of platinum black (2–30 $m^2\ g^{-1}$) [7–9]. It was reported that PEFC performance was greatly improved by efficient utilization of dispersed Pt supported on carbon black rather than platinum black in the catalyst layer [3–7], which suggests that carbon support is essential to achieve high performance in the PEFC. Voltage loss in the PEFC nevertheless remains large: 0.4–0.5 V at a current density of 1 A cm^{-2} [3].

Although PEFC electrocatalysts using carbon black as supports have been studied extensively, there had been previously few studies on PEFC electrocatalysts using carbon materials other than carbon black. Recently, however, electrocatalysts have been prepared by using newly developed nanosize carbon materials, such as carbon nanotubes [10–13], carbon nanohorns [10,14], and carbon nanofibers [15–19]. In contrast to these cutting-edge materials, activated carbon is one of the traditional carbon materials, but it was recently revealed that, by using new techniques, application of activated carbon as a support of electrocatalysts for PEFC had the possibility to improve PEFC performance [20,21].

Activated carbon is easily available, and can be produced from a variety of raw material sources, including waste materials such as waste wood and textiles [22–24], which is a possible advantage of using activated carbon. The high surface area of activated carbon is advantageous for Pt dispersion,

* Corresponding author. Tel.: +81 6 6963 8043; fax: +81 6 6963 8049.
E-mail address: maruyama@omtri.city.osaka.jp (J. Maruyama).

0378-7753/$ – see front matter © 2005 Elsevier B.V. All rights reserved.
doi:10.1016/j.jpowsour.2005.01.040

since it was shown that the specific surface area of the dispersed Pt increases in accordance with that of the carbon black support [25]. The high surface area is also favorable for Pt particles to function independently without interference from neighboring Pt particles. The main drawback of using activated carbon as a support of electrocatalysts for PEFC would be the minute pore diameter, sub-nanometer to nanometer range, which results in slow mass-transfer in the pores of activated carbon, retarding the activity of the electrocatalyst. However, we recently found that the adsorption of trifluoromethanesulfonic acid (CF_3SO_3H) in the pores of activated carbon overcame the problem and significantly enhanced the activity of a catalyst layer formed from activated carbon loaded with Pt (Pt/AC) for O_2 reduction; approximately an eight-fold increase at most, compared to a conventional catalyst layer formed from Pt/carbon black (Pt/C), and attained a 0.1–0.15 V improvement in electrode potential [21].

Activated carbon has various pore structures depending on the raw materials, carbonization conditions, and activation processes. In the preceding study, we investigated the influence of the pore structure on O_2 reduction at the catalyst layer supported on a rotating disk electrode [26]. We formed catalyst layers from activated carbon of various specific surface areas and mean pore diameters by mixing them with the polymer electrolyte. We found that increases in the specific surface area and mean pore diameter increased the activity and that the latter was more effective than the former mainly due to the enhanced mass-transfer in the pores; the catalyst layer formed from activated carbon with the largest mean pore diameter was the most active. Trifluoromethanesulfonic acid was not used in this study to clarify the influence of the pore structure without the influence of its adsorption in the pores.

Adsoption behavior is dependent on the properties of activated carbon. Optimization of the catalyst layer formation, both by selecting properly activated carbon and by adjusting conditions of CF_3SO_3H adsorption fitted to specified activated carbon, would further improve the activity for O_2 reduction, which leads to improvement of PEFC performance. In the present study, we formed catalyst layers from various activated carbons with CF_3SO_3H adsorbed in the pores and investigated the enhancement effect of CF_3SO_3H on O_2 reduction. We found that the oxygen reduction behavior, and consequently the effect, was clearly dependent on the kinds of activated carbon.

2. Experimental

2.1. Materials

Four kinds of activated carbon were used in the present study. For convenience, they are hereafter called AC-1, AC-2, AC-3, and AC-4. The specific surface areas determined by Brunauer–Emmet–Teller (BET) plot, pore volumes, and mean pore diameters of AC-*m* (*m* = 1–4) using the adsorption isotherms of nitrogen onto AC-*m* are shown in Table 1, where the mean pore diameter was calculated assuming the pores to be cylindrical and using the equation

$$d = 4V_p/S$$

where d is the mean pore diameter, V_p the pore volume, and S the specific surface area. Hydrogen hexachloroplatinate hexahydrate ($H_2PtCl_6{\cdot}6H_2O$, Wako Chemical) and sodium tetrahydroborate ($NaBH_4$, Kanto Chemical, 98%) were dissolved in ethanol (dehydrated, Kanto Chemical, reagent grade) to prepare 0.2 and 1 M solutions, respectively, which were used for the platinum loading on the activated carbon. High-purity water was obtained by circulating ion-exchanged water through an Easypure water-purification system (Barnstead, D7403). Perchloric acid (70%, Tama Chemical, analytical grade) was diluted with the high-purity water to prepare 0.1 M $HClO_4$. Nafion® solution [equivalent weight (molar mass per mol of ion-exchange site) = 1100, 5 wt.% dissolved in a mixture of lower aliphatic alcohols and 15–20% water] was purchased from Aldrich. Potassium trifluoromethanesulfonate (CF_3SO_3K, Tokyo Kasei) was used as received and dissolved in the high-purity water. Argon and oxygen gases were of ultra high-purity.

Table 1
Pore structure and adsorption constants for CF_3SO_3K of the activated carbon used as the support of Pt

Activated carbon	AC-1	AC-2	AC-3	AC-4
Specific surface area ($m^2\,g^{-1}$)	1038	1831	1187	1467
Pore volume ($mm^3\,g^{-1}$)	460	839	724	1149
Mean pore diameter (nm)	1.77	1.83	2.25	3.13
K	5.85	9.28	5.94	13.8
N	1.56	1.80	1.58	1.63

The adsorption constants were determined by the Freuntlich equation $\log X = \log K + \left(\frac{1}{N}\right) \log c$ where X ($mg\,g^{-1}$) is the amount of compound adsorbed onto activated carbon of unit mass, c ($g\,dm^{-3}$) the equilibrium concentration of CF_3SO_3K.

2.2. Platinum loading on activated carbon

Platinum was loaded on the activated carbon according to the method reported by Brown and Brown [27]. A 70.2 ± 0.1 mg sample of activated carbon and 0.2 ml of 0.2 M H_2PtCl_6 ethanol solution were added to 4 ml of ethanol. After shaking for 2 days, 1 ml of 1 M $NaBH_4$ ethanol solution was added to the mixture under an Ar atmosphere to produce 10 wt.% Pt/AC. When the activated carbon was AC-*m*, the obtained catalyst was represented as Pt/AC-*m*.

2.3. Catalyst layer formation

A 11.1 ± 0.1 mg sample of Pt/AC-*m* was added to 0.5 ml of the CF_3SO_3K aqueous solution and ultrasonically dispersed. We used the potassium salt instead of CF_3SO_3H to avoid handling the superacid for easier operation. After centrifuging the

mixture, the supernatant was removed. A 10.0 ± 0.1 mg sample of carbon black (Vulcan XC-72R, Cabot) as an electron-conductive agent and 1 ml of the Nafion® solution were added to the deposited CF_3SO_3K-adsorbed Pt/AC-*m*, and the mixture was ultrasonically dispersed to give a catalyst paste [21,28]. A glassy carbon rotating disk electrode (GC RDE, Hokuto Denko), which consisted of a GC rod sealed in a Kel-F holder, was polished with a 2000 grit emery paper (Sumitomo 3M) and then ultrasonically cleaned in high-purity water for use as a support for the catalyst layer. The geometric surface area of the electrode was 0.196 cm^2 (diameter 5 mm). Three μl of the paste was pipetted onto the GC surface, and, to shield it from the irregular air stream generated by a ventilator, the electrode was immediately placed under a glass cover until the layer was formed. After removing the glass cover, the electrode was further dried overnight at room temperature. Potassium cation in the catalyst layer was replaced by H^+ by immersing the layer in 0.1 M $HClO_4$ before evaluation of the electrochemical properties of the layer. Catalyst layers without CF_3SO_3H were formed in the same way as described above except using 0.5 ml of the highly pure water instead of CF_3SO_3K solutions in the CF_3SO_3K adsorption step.

2.4. Adsorption isotherm of CF_3SO_3K onto activated carbon

An aliquot of 50.0 ± 0.1 mg of AC-*m* was added to 0.5 ml (for *m* = 1–3) or 1.0 ml (for *m* = 4) of the CF_3SO_3K aqueous solution in a glass tube with a screw cap. The concentration of CF_3SO_3K was varied in the range of 0.05–4.0 M. After dispersing Pt/AC-*m* ultrasonically, the tube was left in a water bath at 25 °C. The equilibrium concentration of CF_3SO_3K was determined by measuring the ionic conductivity of the supernatant with a conductivity meter (Model CM-2A, Toa Electron) and by using the conductivity–concentration relationship that was obtained in advance by measuring the conductivity of the same solutions in the absence of AC-*m*. The amount of CF_3SO_3K adsorbed onto AC-*m* was calculated from the difference between the concentration of CF_3SO_3K before and after adsorption.

2.5. Electrochemical measurements

An automatic polarization system (HZ-3000, Hokuto Denko) and an RDE apparatus (HR-201, Hokuto Denko) equipped with a glass cell were used for the cyclic voltammetry and the measurement of current-potential relations. The glass cell was cleaned by soaking in a 1:1 mixture of concentrated HNO_3 and H_2SO_4, followed by a thorough rinsing with high-purity water and finally steam-cleaning [29]. The counter electrode was a Pt wire and the reference electrode was a reversible hydrogen electrode (RHE). All potentials were referred to the RHE. Cyclic voltammograms for the catalyst layers were recorded in 0.1 M $HClO_4$ at 25 °C. The potential was scanned between 0.05 and 1.3 V at a scan rate of 50 mV s^{-1}. Before recording, the potential was repeatedly scanned between 0.05 and 1.4 V to remove the residual impurities. Current-potential relations were measured in O_2-saturated 0.1 M $HClO_4$ at 25 °C at various rotation speeds. The scan rate of the potential was fixed at 10 mV s^{-1}. Prior to the measurements, the electrode was repeatedly polarized at 0.05 and 1.3 V alternately [30]. The potential was finally stepped to 0.2 V and then swept in the positive direction from 0.2 to 1.2 V to obtain the current-potential relationship. The background current was similarly measured in an Ar atmosphere without rotation.

3. Results and discussion

3.1. Adsorption of CF_3SO_3K onto activated carbon

The adsorption isotherms of CF_3SO_3K onto AC-1, AC-2, and AC-4 at 25 °C are shown in Fig. 1. The adsorption isotherm of CF_3SO_3K onto AC-3 was almost the same as that onto AC-1. The isotherms confirmed CF_3SO_3K adsorption onto AC-*m*. It has been recognized that adsorption of organic compounds onto activated carbon in aqueous solutions often follows the Freundlich equation [31]

$$\log X = \log K + \left(\frac{1}{N}\right) \log c$$

where *X* is the amount of compound adsorbed onto activated carbon of unit mass, *c* the equilibrium concentration, and *K* and *N* are the adsorption constants. The relationships between the amount of adsorbed CF_3SO_3K and the equilibrium concentration also followed this equation for all activated carbons used in the present study. The values of *K* and *N*, estimated by linear regression analysis, are listed in Table 1. They are smaller than those for adsorption of common organic compounds [32], indicating low affinity between CF_3SO_3K and activated carbon, which is expected from the fact that adsorption onto a carbon surface, whose surface is hydrophobic, is mainly caused by the London dispersion force and that CF_3SO_3K is highly soluble in water. However, the hydrophobic CF_3 group might contribute to the adsorption onto

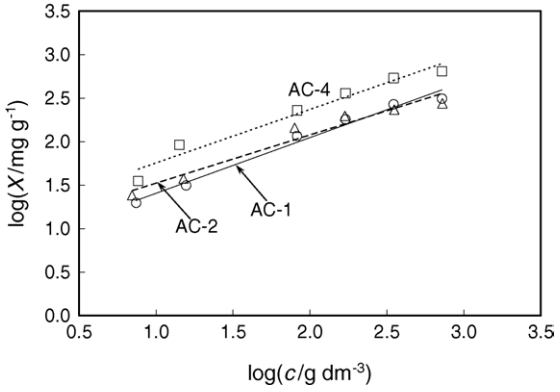

Fig. 1. The adsorption isotherms of CF_3SO_3K onto AC-1 (◯), AC-2 (△), and AC-4 (□) at 25 °C.

the activated carbon. CF_3SO_3K was presumably adsorbed on the surface with the group orientated toward the surface [33].

The values of K and N varied when the kinds of activated carbon changed. It has been recognized that they increase with an increase in an affinity for the adsorbent and K increases also with an increase in adsorption capacity of the activated carbon [31]. Adsorption capacity generally increases with an increase in the specific surface area of the activated carbon, which might result in the almost same K for AC-1 as AC-3, and on the larger value for AC-2 than for AC-1. The surface chemical states also influence K and N, which might be the reason for the further increase in K for AC-4, although details in the influence of surface states of activated carbon has not been clarified yet.

3.2. Electrochemically active surface area in Pt/AC

Fig. 2 shows the cyclic voltammograms for the catalyst layers formed from Pt/AC-*m* in Ar-saturated 0.1 M $HClO_4$. The current was generated only from the surface that was in contact with Nafion® CF_3SO_3H, the electrochemically active surface, and was mostly attributable to the double-layer charging of the activated carbon surface and the redox reaction of the quinone-like surface functional groups [34]. The peaks caused by the Pt surface reactions were reduced by the overlapping of these currents or by the loss in the crystal faces due to dispersion [20,35,36]. It was impossible to determine the Pt surface area from the charge caused by the hydrogen adsorption and desorption. However, it could be assumed that the surface functional groups and Pt were almost uniformly distributed in the Pt/AC pores [26]. The charge, which corresponds to the enclosed area in the voltammogram is, therefore, nearly proportional to the electrochemically active surface area.

If Nafion® molecules fully penetrated into the pores and the entire surface in the Pt/AC pores was in contact with Nafion®, the ideal state, the electrochemically active surface area would be exactly proportional to the specific surface area of the Pt/AC, although this state is not practically realized. This deviation from the ideal state might be pronounced with an activated carbon of small pore diameter, which is disadvantageous to the penetration of Nafion® molecules. The deviation would occur also with an activated carbon of large specific surface area. Increase in specific surface area implies development of pores inside a carbon particle. The penetration of Nafion® molecules into the pores proceeds at a finite speed, and stops once the molecules are held in the middle of the pore [37]. Thus, the part of the pore surface not in contact

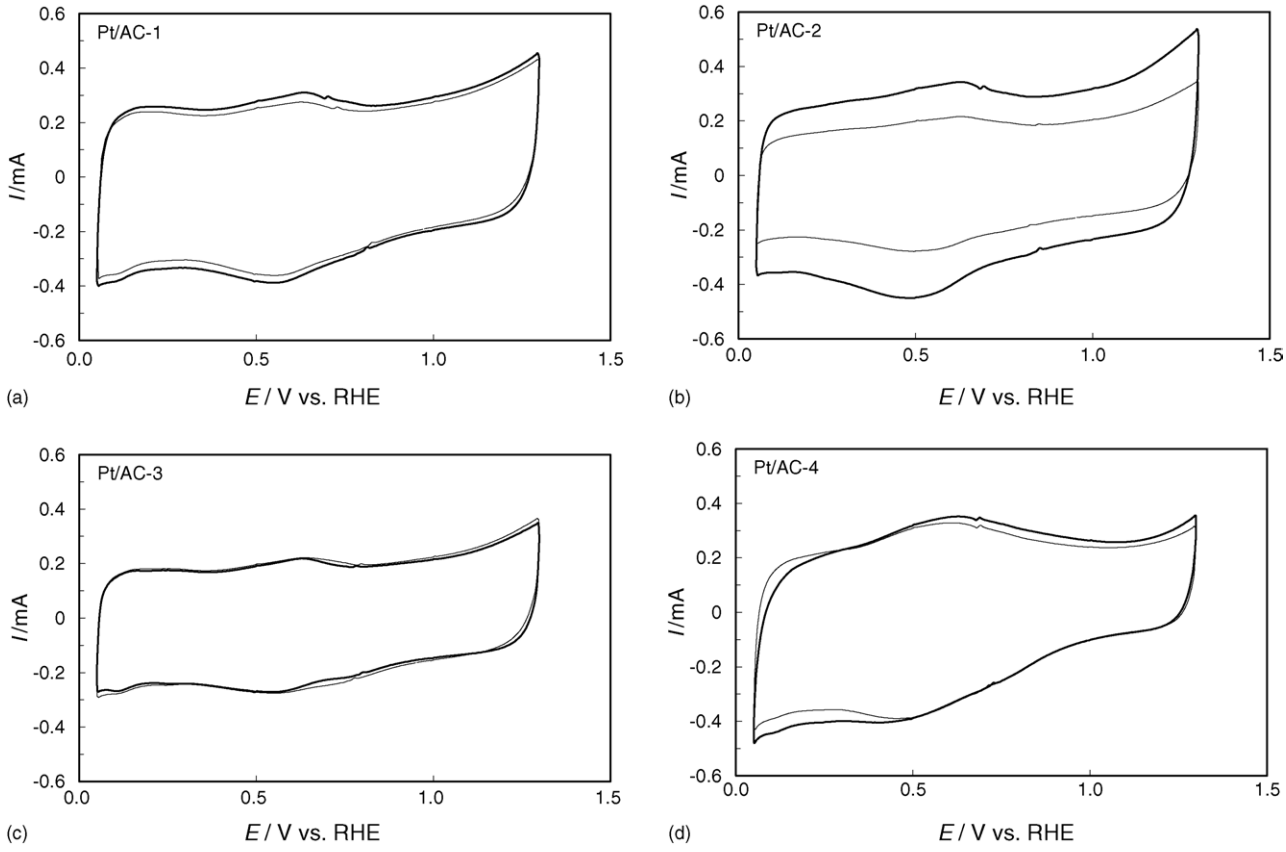

Fig. 2. Cyclic voltammograms for catalyst layers formed from (a) Pt/AC-1, (b) Pt/AC-2, (c) Pt/AC-3, and (d) Pt/AC-4 supported on GC RDE in Ar-saturated 0.1 M $HClO_4$. Scan rate: 50 mV s^{-1}. The voltammograms for the catalyst layers without CF_3SO_3H are displayed in thin lines, and those for the layers containing CF_3SO_3H are displayed in thick lines. Concentration of CF_3SO_3K solution used for its adsorption was 4.0 M.

with Nafion® would increase with an increase in the extent of the pore development.

The charge increased by the adsorption of CF_3SO_3H at the Pt/AC-1, Pt/AC-2, and Pt/AC-4 layers, by a factor of 1.08, 1.58, and 1.04, respectively, but decreased at the Pt/AC-3 layer by a factor of 0.97. The decrease was caused by blocking of the pore surface of activated carbon by the CF_3SO_3H adsorption. On the contrary, the increase was caused by the presence of CF_3SO_3H in the depths of the pores and function of CF_3SO_3H as an electrolyte, attributable to easier penetration of CF_3SO_3K than that of Nafion® molecules into the pore of activated carbon. At the Pt/AC-1, Pt/AC-2, and Pt/AC-4 layers, the increase due to the CF_3SO_3K penetration exceeded the decrease due to the surface blocking by the CF_3SO_3H adsorption, which resulted in the enlargement of the electrochemically active surface area in total. The enlargement was most pronounced at the Pt/AC-2 layer, as expected from the largest surface area among the activated carbons used in this study. At the Pt/AC-3 layer, the increase due to the CF_3SO_3K penetration was lacking for compensating the decrease due to the surface blocking by the CF_3SO_3H adsorption, which resulted in the decrease in the charge which corresponds to the enclosed area in the voltammogram in total, despite the similar specific surface area of AC-3 to AC-1. This result might be attributed to the increase in the mean pore diameter compared to AC-1, which allows the penetration of Nafion® molecules nearly as deeply as that of the CF_3SO_3K penetration. Thus, the increase in the electrochemical active surface area due to the CF_3SO_3K penetration became small, and consequently the charge, which corresponds to the enclosed area in the voltammogram, decreased. The smaller increase in the active surface area at the Pt/AC-4 layer was also attributable to the large mean pore diameter of AC-4.

3.3. Cathodic oxygen reduction at catalyst layers

Oxygen reduction currents at the catalyst layers, I, were measured in O_2-saturated 0.1 M $HClO_4$ with the electrodes rotated at various speeds. Fig. 3 shows typical relationships between the electrode potential and the current at the Pt/AC-4 layers with CF_3SO_3H adsorbed from the CF_3SO_3K solutions of various concentrations. The sign of the current due to reduction reactions was taken as negative. The O_2 reduction current shown in Fig. 3 was obtained by subtracting the background current from the measured current. Although the oxygen reduction currents at the layers formed by using 1 and 2 M CF_3SO_3K were smaller than that at the CF_3SO_3H-free layer between 0.6 and 0.9 V, the current increased almost corresponding to an increase in the CF_3SO_3K concentration. The behavior was dependent on the kind of activated carbon.

The current shown in Fig. 3 arose from O_2 reduction inside the catalyst layer, but included the influence of mass-transfer in 0.1 M $HClO_4$ solution in which the catalyst layer was immersed. The activities of the catalyst layers for O_2 reduction were evaluated using the reduction current free of the influence of mass-transfer in the solution, I_K, determined by the

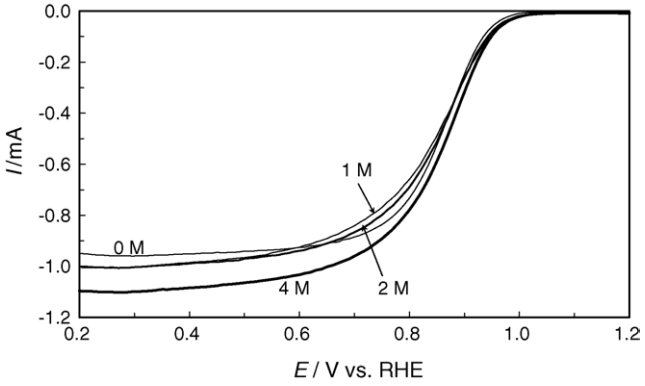

Fig. 3. Current-potential relationship of positive scans for O_2 reduction at catalyst layers formed from Pt/AC-4 with CF_3SO_3H adsorbed in the pores. Concentrations of CF_3SO_3K solutions used for its adsorption were 0 M (very thin line), 1 M (thin line), 2 M (thick line), and 4 M (very thick line). Scan rate: 10 mV s^{-1}. Electrode-rotation speed: 2000 rpm.

equation shown below [20,21,28,38].

$$-\frac{1}{I} = -\frac{1}{I_K} + \frac{1}{0.620nFAD^{2/3}c\nu^{-1/6}\omega^{1/2}}$$

where n is the number of electrons involved in O_2 reduction per molecule, F the Faraday constant, A the geometric area of the GC electrode, D the diffusion coefficient of O_2 in solution, c the concentration of O_2 in solution, ν the kinematic viscosity of the solution, and ω the angular frequency of the rotation. Fig. 4 shows typical $-1/I$ versus $\omega^{-1/2}$ plots for O_2 reduction at the Pt/AC-4 layers with CF_3SO_3H adsorbed from the CF_3SO_3K solutions of various concentrations. The number of electrons involved in O_2 reduction per molecule, n, can be calculated by using the slope of the plot and the following values [37,39,40]: F, 96485 C mol^{-1}; A, 0.0707 cm^2; D, 1.9×10^{-5} cm^2 s^{-1}; c, 1.18×10^{-6} mol cm^{-3}; ν, 9.87×10^{-3} cm^2 s^{-1}. Two-electron reduction generates intermediate H_2O_2 (reaction 1). Increase in n occurs with its further reduction (reaction 2), decomposition of H_2O_2 (reaction 3), or increase in the propor-

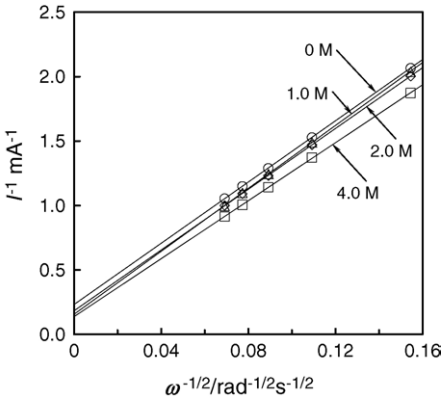

Fig. 4. $-1/I$ vs. $\omega^{-1/2}$ plots for O_2 reduction at catalyst layers formed from Pt/AC-4 with CF_3SO_3H adsorbed in the pores. Concentrations of CF_3SO_3K solutions used for its adsorption were 0 M (◯), 1 M (△), 2 M (◊), and 4 M (□). Electrode potential: 0.2 V.

tion of four-electron reduction to H_2O (reaction 4) [41,42].

$$O_2 + 2H^+ + 2e^- \rightarrow H_2O_2 \quad (1)$$

$$H_2O_2 + 2H^+ + 2e^- \rightarrow 2H_2O \quad (2)$$

$$2H_2O_2 \rightarrow 2H_2O + O_2 \quad (3)$$

$$O_2 + 4H^+ + 4e^- \rightarrow 2H_2O \quad (4)$$

The n value close to 4 is preferred for PEFC to promote efficiency and long-term duability since H_2O_2 damages the polymer electrolyte. Although the n values calculated from the results shown in Fig. 4 were scattered from 3.4 to 3.7, the average of the four results was 3.6, nearly four, indicating that most O_2 molecules were reduced to H_2O, irrespective of the presence of CF_3SO_3H [21]. As for n, similar behavior was observed at the catalyst layers formed from the other activated carbons.

3.4. Effect of CF_3SO_3H adsorption on activity for oxygen reduction at catalyst layers

The dependency of electrochemical properties on the kind of activated carbon was observed for the relationships between the electrode potential, E, and I_K for O_2 reduction at catalyst layers formed from Pt/AC-m, shown in Fig. 5. In Fig. 5(a) for the Pt/AC-1 layer, the maximum performance was obtained when the concentration of the CF_3SO_3K solution used in its adsorption step was 1 M. At the Pt/AC-2 layer (Fig. 5(b)), CF_3SO_3H adsorption enhanced the activity and the enhancement was nearly equal in the low potential region. The enhancement of the activity was larger at the Pt/AC-3 layer (Fig. 5(c)) than at the Pt/AC-2 layer and was further enlarged at the Pt/AC-4 layer (Fig. 5(d)), although the activity was lower at the layers formed by using 1 and 2 M CF_3SO_3K than that at the CF_3SO_3H-free layer between 0.55 and 0.8 V. The addition of CF_3SO_3K might possibly change distribution of the particles in the Pt/AC-4 layer to result in the activity decrease, which was associated with the adsorption isotherm apart from those for Pt/AC-1, 2, and 3, shown in Fig. 1, although the reason for the decrease is not fully explicable at present.

The enhancement in the low potential region is mainly attributable to enhancement of the mass-transfer in the Pt/AC pores; i.e. O_2 diffusion and H^+ migration [21]. That in the high potential region is mainly attributable to the increase in the kinetic, intrinsic activity of the Pt/AC particle for O_2 reduction, caused by, for instance, increase in Pt utilization and Pt dispersion, and partly to the enhancement of the mass-transfer in the pores [20,26]. In the intermediate potential region, the contribution of the effect of mass-transfer enhancement increases with a decrease in the electrode potential. At 0.9 V, the ratio of $-I_K$ at the Pt/AC-m layers with CF_3SO_3H adsorbed using 4.0 M CF_3SO_3K solution to that at the layers without it were: 1.32, $m = 1$; 1.59, $m = 2$; 1.09, $m = 3$; 1.60,

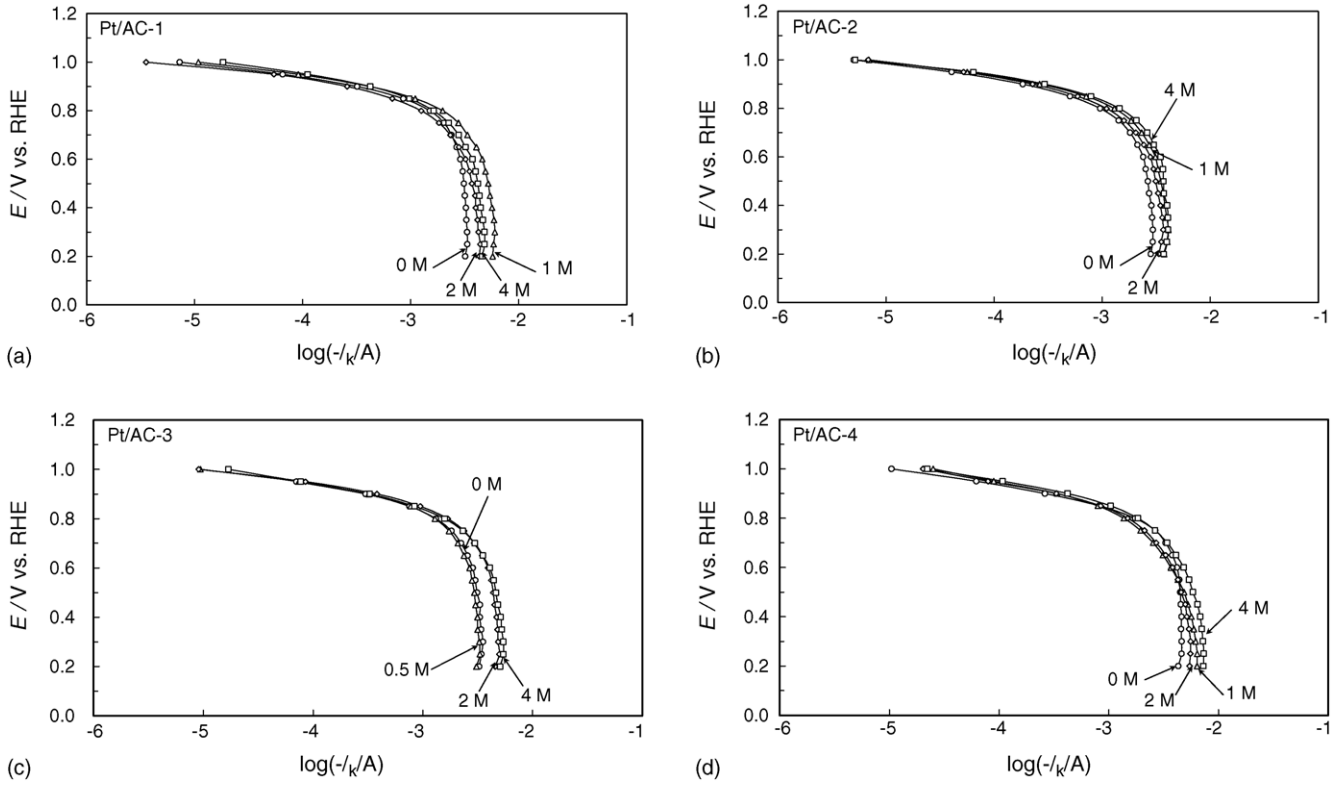

Fig. 5. Tafel plots of I_K for O_2 reduction at catalyst layers formed from (a) Pt/AC-1, (b) Pt/AC-2, (c) Pt/AC-3, and (d) Pt/AC-4. Concentrations of CF_3SO_3K solutions used for its adsorption are indicated inside the figure.

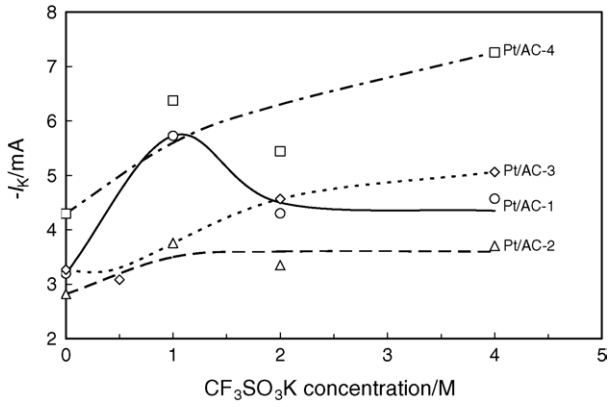

Fig. 6. Dependency of I_K at 0.2 V (start of positive scan) on concentration of CF_3SO_3K solution used for its adsorption at catalyst layers formed from Pt/AC-1 (◯), Pt/AC-2 (△), Pt/AC-3 (◇), and Pt/AC-4 (□).

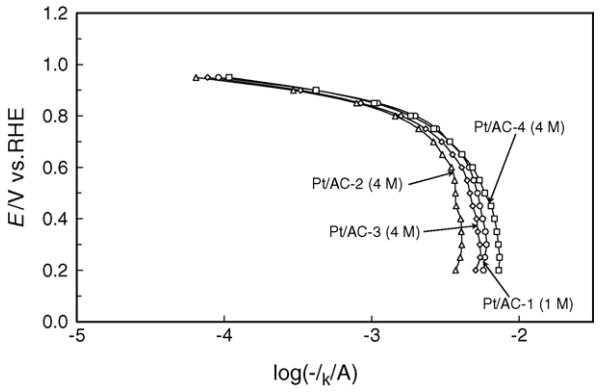

Fig. 7. Tafel plots of I_K for O_2 reduction at catalyst layers exhibiting the maximum performance at each kind of activated carbon: Pt/AC-1 (◯); Pt/AC-2 (△); Pt/AC-3 (◇); Pt/AC-4 (□). Concentrations of CF_3SO_3K solutions used for its adsorption are indicated in parentheses.

$m = 4$. Since the oxygen reduction current at the high potential such as 0.9 V included somewhat large error due to the smallness of the current, we compared $-I_K$ at the layer without CF_3SO_3H only to that with CF_3SO_3H adsorbed using the most concentrated CF_3SO_3K solution, presuming that the difference might be the most clearly observed. The increase in $-I_K$ at the Pt/AC-1 and Pt/AC-2 layers were in agreement with the increase in the electrochemically active surface area, and consequently, the Pt utilization. At the Pt/AC-3 and Pt/AC-4 layers with the increase in the area absent or small, the increase in $-I_K$ was due to the enhancement of the mass-transfer. The dependency of I_K at 0.2 V on the concentration of the CF_3SO_3K solution used for its adsorption at catalyst layers is shown in Fig. 6. The potential was chosen for demonstrating the effect of the mass-transfer enhancement the most clearly. At the Pt/AC-1 layer, $-I_K$ reached the maximum when the concentration of the CF_3SO_3K solution was 1 M, and decreased with a further increase in the concentration. At the Pt/AC-2 layer, $-I_K$ increased by the CF_3SO_3H adsorption, but remained constant despite the increase in the concentration above 1 M. In contrast, $-I_K$ kept increasing with the concentration increase at the Pt/AC-3 layer. This upward tendency was promoted at the Pt/AC-4 layer although the points were scattered to some extent.

These dependencies could be associated with the pore volumes of the activated carbons and the adsorption behaviors of CF_3SO_3K. The decrease in $-I_K$ after reaching the maximum was only observed at the Pt/AC-1 layer. It could be assumed that the concentration of CF_3SO_3H in the pores was optimized when $-I_K$ reached the maximum. The pore volume of AC-1 was the smallest among the activated carbons used in the present study. When the concentration of the CF_3SO_3K solution exceeded 1 M, an excessive amount of CF_3SO_3H might be present at the Pt/AC-1, probably near the outer surface of the Pt/AC-1 particle with its inside occupied. The decrease in $-I_K$ was thus attributable to the decrease in electron-conduction in the Pt/AC-1 layer due to the excess CF_3SO_3H that blocked contact with the carbon black [20]. The other activated carbons possessed larger pore volume than AC-1, which would imply that the CF_3SO_3H concentrations were less than the optimized value. It should be noted that the exact CF_3SO_3H concentration in the pore could not determined here since the pore volume determined by the N_2 adsorption isotherm was only the value for the pores whose pore diameter was below 30 nm and CF_3SO_3H would be present in the pores of larger pore diameter. Nevertheless, the former pores were crucial for the electrochemical properties of the catalyst layers, which was indicated by the behavior shown in the cyclic voltammograms and by our preceding study [26].

Fig. 7 shows Tafel plots of I_K for O_2 reduction at the catalyst layers exhibiting the maximum performance at each kind of activated carbon. The activity of the Pt/AC-1 layer was higher than those of the Pt/AC-2 and Pt/AC-3 layers owing to the absence of excessive pore development, avoiding loss of connection between the activated carbon and the electron-conductive agent in the catalyst layer [26]. The maximum performance was obtained at the Pt/AC-4 layer despite its highly developed pores, by exceeding this disadvantage, probably due to the efficient enhancement of the mass-transfer by CF_3SO_3H in the pores of the largest mean pore diameter among those for the activated carbons used in the present study. Although the CF_3SO_3K concentration in aqueous solution is limited, the activity would be further improved by findings of methods to increase the amount of CF_3SO_3H in the pores. Optimization of the content of carbon black in the catalyst layers would also improve the activity, since the optimum content of carbon black might be dependent on the amount of CF_3SO_3H adsorbed on Pt/AC.

4. Conclusions

Catalyst layers were formed from activated carbons of various pore structure with Pt loaded and CF_3SO_3H adsorbed in the pores, and were investigated for their activity for oxygen reduction by supporting the layer on GC RDEs. Introduction of CF_3SO_3H into the catalyst layer was carried out by

CF_3SO_3K adsorption onto the activated carbon followed by replacing K^+ with H^+ to avoid handling the superacid for easier operation. The adsorption was confirmed by the adsorption isotherm of CF_3SO_3K onto the activated carbon, which was dependent on the kind of the activated carbon. Electrochemical properties of the catalyst layer were also dependent on it. The electrochemical active surface area of the layer, evaluated by cyclic voltammetry, was influenced by two factors: decrease by surface blocking due to the adsorbed CF_3SO_3H; increase by the presence of CF_3SO_3H in the depths of the pores, attributable to easier penetration of CF_3SO_3K than that of Nafion® molecules into the pores of the activated carbon. The relative importance between these effects was dependent on the pore structure of the activated carbon. The area was associated with the activity of the layer for O_2 reduction in the high potential region. Dependencies of the activity on the concentration of the CF_3SO_3K solution in the low potential region suggested the necessity of concentration adjustment for the effective enhancement of the mass-transfer in the pores of the activated carbon, according to the pore structure. The maximum performance was obtained at the layer formed from the activated carbon with the largest pore diameter and modest specific surface area among the activated carbons, with CF_3SO_3K adsorbed from the most concentrated solution, used in this study, which indicates that the activated carbon of wide pore containing the optimum amount of CF_3SO_3H would be promising for improvement of PEFC performance.

Acknowledgement

We thank Mr. I. Takahashi for his help with the experiments.

References

[1] D.M. Bernardi, M.W. Verbrugge, J. Electrochem. Soc. 139 (1992) 2477–2491.
[2] M. Watanabe, M. Uchida, S. Motoo, J. Electroanal. Chem. 229 (1987) 395–406.
[3] S. Gottesfeld, T.A. Zawodzinski, in: R.C. Alkire, H. Gerischer, D.M. Kolb, C.W. Tobias (Eds.), Advances in Electrochemical Science and Engineering, vol. 5, Wiley-VCH, Weinheim, 1997, p. 195.
[4] K. Kinoshita, Electrochemical Oxygen Technology, Wiley, New York, 1992.
[5] M.S. Wilson, S. Gottesfeld, J. Appl. Electrochem. 22 (1992) 1–7.
[6] M.S. Wilson, S. Gottesfeld, J. Electrochem. Soc. 139 (1992) L28–L30.
[7] P. Costamagna, S. Srinivasan, J. Power Sources 102 (2001) 242–252.
[8] A.M. Feltham, M. Spiro, Chem. Rev. 71 (1971) 177–193.
[9] J. Bett, J. Lundquist, E. Washington, P. Stonehart, Electrochim. Acta 18 (1973) 343–348.
[10] H. Shioyama, K. Yasuda, Tanso 210 (2003) 236.
[11] W. Li, C. Ling, W. Zhou, J. Qiu, Z. Zhou, G. Sun, Q. Xin, J. Phys. Chem. B 107 (2003) 6292.
[12] B. Rajesh, K.R. Thampi, J.-M. Bonard, N. Xanthopoulos, H.J. Mathieu, B. Viswanathan, J. Phys. Chem. B 107 (2003) 2701.
[13] W. Li, C. Ling, J. Qiu, W. Zhou, H. Han, Z. Wei, G. Sun, Q. Xin, Carbon 40 (2002) 791.
[14] T. Yoshitake, Y. Shimakawa, S. Kuroshima, H. Kimura, T. Ichihashi, Y. Kubo, D. Kasuya, K. Takahashi, F. Kokai, M. Yudasaka, S. Iijima, Physica B 323 (2002) 124.
[15] E.S. Steigerwalt, G.A. Deluga, C.M. Lukehart, J. Phys. Chem. B 106 (2002) 760.
[16] E.S. Steigerwalt, G.A. Deluga, D.E. Cliffel, C.M. Lukehart, J. Phys. Chem. B 105 (2001) 8097.
[17] C.A. Bessel, K. Laubernds, N.M. Rodriguez, R.T.K. Baker, J. Phys. Chem. B 105 (2001) 1115.
[18] G. Che, B.B. Lakshmi, C.R. Martin, E.R. Fisher, Langmuir 15 (1999) 750.
[19] G. Che, B.B. Lakshmi, E.R. Fisher, C.R. Martin, Nature 393 (1998) 346.
[20] J. Maruyama, I. Abe, Electrochim. Acta 48 (2003) 1443.
[21] J. Maruyama, I. Abe, J. Electrochem. Soc. 151 (2004) 447.
[22] S. Iwasaki, T. Fukuhara, I. Abe, J. Yanagi, M. Mouri, Y. Iwashima, T. Tabuchi, O. Shinohara, Synth. Met. 125 (2002) 207.
[23] S. Iwasaki, T. Fukuhara, Y. Yoshimura, R. Sakaguchi, Y. Shibutani, I. Abe, Sen'I Gakkaishi 57 (2001) 359.
[24] I. Abe, T. Fukuhara, J. Maruyama, H. Tatsumoto, S. Iwasaki, Carbon 39 (2001) 1069.
[25] M. Watanabe, H. Sei, P. Stonehart, J. Electroanal. Chem. 261 (1989) 375.
[26] J. Maruyama, K. Sumino, M. Kawaguchi, I. Abe, Carbon 42 (2004) 3115.
[27] H.C. Brown, C.A. Brown, J. Am. Chem. Soc. 84 (1962) 2828.
[28] S.L. Gojković, S.K. Zečević, R.F. Savinell, J. Electrochem. Soc. 145 (1998) 3713.
[29] D. Chu, D. Tryk, D. Gervasio, E.B. Yeager, J. Electroanal. Chem. 272 (1989) 277.
[30] M. Razaq, A. Razaq, E. Yeager, D.D. DesMarteau, S. Singh, J. Electrochem. Soc. 136 (1989) 385.
[31] S. Kondo, T. Ishikawa, I. Abe, Science of Adsorption, Maruzen, Tokyo, 1991.
[32] I. Abe, K. Hayashi, T. Hirashima, M. Kitagawa, J. Am. Chem. Soc. 104 (1982) 6452.
[33] J. Maruyama, I. Abe, Electrochim. Acta 46 (2001) 3381.
[34] C. Barbero, J.J. Silber, L. Sereno, J. Electroanal. Chem. 248 (1988) 321.
[35] J. Maruyama, M. Inaba, K. Katakura, Z. Ogumi, Z. Takehara, J. Electroanal. Chem. 447 (1998) 201.
[36] H. Yoshitake, O. Yamazaki, K. Ota, J. Electrochem. Soc. 141 (1994) 2516.
[37] J. Maruyama, I. Abe, J. Electroanal. Chem. 545 (2003) 109.
[38] U.A. Paulus, T.J. Schmidt, H.A. Gasteiger, R.J. Behm, J. Electroanal. Chem. 495 (2001) 134.
[39] S.K. Zečević, J.S. Wainright, M.H. Litt, S.L. Gojković, R.F. Savinell, J. Electrochem. Soc. 144 (1997) 2973.
[40] R.M.Q. Mello, E.A. Ticianelli, Electrochim. Acta 42 (1997) 1031.
[41] M.R. Tarasevich, A. Sadkowski, E. Yeager, in: J.O. Bockris, B.E. Conway, E. Yeager, S.U.M. Khan, R.E. White (Eds.), Comprehensive Treatise of Electrochemistry, vol. 7, Plenum, New York, 1983 (Chapter 6).
[42] J. Maruyama, M. Inaba, T. Morita, Z. Ogumi, J. Electroanal. Chem. 504 (2001) 208.